Cardiovascular Research (2009) **84**, 387–395
doi:10.1093/cvr/cvp246

Redox modification of ryanodine receptors underlies calcium alternans in a canine model of sudden cardiac death

Andriy E. Belevych[1], Dmitry Terentyev[1], Serge Viatchenko-Karpinski[1], Radmila Terentyeva[1], Arun Sridhar[1,2], Yoshinori Nishijima[1,2], Lance D. Wilson[3], Arturo J. Cardounel[4], Kenneth R. Laurita[3], Cynthia A. Carnes[1,2], George E. Billman[1], and Sandor Gyorke[1]*

[1]*Department of Physiology and Cell Biology, Davis Heart and Lung Research Institute, The Ohio State University, College of Medicine, 473 W. 12th Avenue, Columbus, OH 43210, USA;* [2]*College of Pharmacy, The Ohio State University, Columbus, OH, USA;* [3]*The Heart and Vascular Research Center, Case Western Reserve University, MetroHealth Campus, Cleveland, OH, USA; and* [4]*Department of Physiology, College of Medicine, University of Florida, Gainesville, FL, USA*

Received 22 April 2009; revised 26 June 2009; accepted 13 July 2009; online publish-ahead-of-print 17 July 2009

Time for primary review: 28 days

KEYWORDS
Cardiac alternans;
Ryanodine receptor;
Redox modification;
Ca^{2+} release;
Myocardial infarction

Aims Although cardiac alternans is a known predictor of lethal arrhythmias, its underlying causes remain largely undefined in disease settings. The potential role of, and mechanisms responsible for, beat-to-beat alternations in the amplitude of systolic Ca^{2+} transients (Ca^{2+} alternans) was investigated in a canine post-myocardial infarction (MI) model of sudden cardiac death (SCD).
Methods and results Post-MI dogs had preserved left ventricular (LV) function and susceptibility to ventricular fibrillation (VF) during exercise. LV wedge preparations from VF dogs were more susceptible to action potential (AP) alternans and the frequency-dependence of Ca^{2+} alternans was shifted towards slower rates in myocytes isolated from VF dogs relative to controls. In both groups of cells, cytosolic Ca^{2+} transients ($[Ca^{2+}]_c$) alternated in phase with changes in diastolic Ca^{2+} in sarcoplasmic reticulum ($[Ca^{2+}]_{SR}$), but the dependence of $[Ca^{2+}]_c$ amplitude on $[Ca^{2+}]_{SR}$ was steeper in VF cells. Abnormal ryanodine receptor (RyR) function in VF cells was indicated by increased fractional Ca^{2+} release for a given amplitude of Ca^{2+} current and elevated diastolic RyR-mediated SR Ca^{2+} leak. SR Ca^{2+} uptake activity did not differ between VF and control cells. VF myocytes had an increased rate of reactive oxygen species production and increased RyR oxidation. Treatment of VF myocytes with reducing agents normalized parameters of Ca^{2+} handling and shifted the threshold of Ca^{2+} alternans to higher frequencies.
Conclusion Redox modulation of RyRs promotes generation of Ca^{2+} alternans by enhancing the steepness of the Ca^{2+} release–load relationship and thereby providing a substrate for post-MI arrhythmias.

1. Introduction

Sudden cardiac death (SCD) due to sustained ventricular arrhythmias [ventricular tachycardia or ventricular fibrillation (VF)] is a major cause of mortality in patients following myocardial infarction (MI).[1–3] In these patients, ventricular ectopy appears to be part of the pathogenic mechanism of arrhythmias, whereas electrical heterogeneity and dispersion of repolarization are thought to be essential for the arrhythmogenic substrate.[4] One important source of repolarization dispersion is cardiac alternans, a beat-to-beat alternation in action potential duration (APD) and contractile force or intracellular Ca^{2+} transient.[5,6] Ca^{2+} dynamics, and in particular regulation of Ca^{2+} release from the sarcoplasmic reticulum (SR), has been recognized as a key factor in the genesis of electromechanical alternans.[6–9]

Several factors have been implicated in the disturbances of Ca^{2+} signalling that result in alternans. These include slowed SR Ca^{2+} uptake,[10,11] incomplete recovery of ryanodine receptor (RyR) from inactivation,[12,13] and increased steepness of the Ca^{2+} release–SR Ca^{2+} content relationship.[11,14] However, the relative importance of these factors in the genesis of alternans remains a subject of debate. Moreover, most studies of alternans have been performed in myocytes from healthy hearts using various experimental interventions or computer simulations using mathematical models of Ca^{2+} cycling. Thus, the mechanisms of alternans in clinically relevant disease models remain largely unexplored.

* Corresponding author. Tel: +1 614 292 3969; fax: +1 614 247 7799.
E-mail address: sandor.gyorke@osumc.edu

Altered redox balance and redox-mediated changes in Ca^{2+} handling are increasingly recognized as important pathogenic factors in different cardiac diseases, including both ischaemic and non-ischaemic disease processes.[15] Reactive oxygen species (ROS) have the capability to affect Ca^{2+} handling via redox modification of components of the excitation–contraction (EC) coupling machinery, including RyRs.[16] However, the potential role of redox-mediated alterations of Ca^{2+} signalling in the genesis of alternans and arrhythmias in general remains to be investigated.

In the present study, the potential role of, and mechanisms responsible for, Ca^{2+} alternans was investigated using a canine post-MI model of SCD. This well-characterized model is known to recapitulate many aspects of humans with healed MIs and a residual risk of SCD (recently reviewed in Billman[17]) including altered repolarization, altered autonomic balance, and responses to pharmacological interventions. The present study reports susceptibility to Ca^{2+} alternans at the tissue and myocyte levels in post-MI animals with a demonstrated vulnerability to sustained ventricular tachycardia and VF. Ca^{2+} alternans resulted from the increased steepness of the SR Ca^{2+} release–content relationship and is attributable to enhanced RyR activity secondary to redox modification of the channel protein.

2. Methods

Expanded Methods section is given in Supplementary material online.

2.1 Canine model of sustained ventricular tachyarrhythmia

All *in vivo* procedures[18,19] were approved by the Ohio State University Institutional Animal Care and Use Committee and conformed with the *Guide for the Care and Use of Laboratory Animals* published by the US National Institutes of Health (NIH Publication No. 85-23, revised 1996). An anterior wall MI was induced by ligation of the left anterior descending coronary artery, and a vascular occluder was placed on the left circumflex coronary artery at the time of surgery. A minimum of 4 weeks after surgery and the MI, the dogs were risk-stratified for arrhythmia susceptibility by an exercise plus ischaemia test as described previously.[17] This test reliably induced ventricular flutter that deteriorated into VF. A minimum of 7 days elapsed between the exercise plus ischaemia test and tissue or myocyte isolation to avoid any acute effects of recent ischaemia. Only dogs with VF in response to the exercise plus ischaemia test were included in the present study (VF animals, $n = 13$ female, age 2–3 years, weight 18–26 kg); a group of 20 normal dogs (male/female, age 1–4 years, weight 15–25 kg) served as controls. Left ventricle (LV) function was assessed in a subset of control and VF animals using echocardiography. For the dogs used in the present study, LV fractional shortening was 41 ± 2 and $41 \pm 1\%$ in control ($n = 10$) and VF ($n = 5$) animals, respectively.[20]

2.2 Optical AP mapping in the canine wedge preparation

Canine wedge preparations were isolated from normal ($n = 4$) and VF (excluding both infracted and border zone tissue, $n = 4$) dogs and placed in an imaging chamber for optical mapping while being perfused with Tyrode solution. Wedges were stained with the voltage-sensitive dye, di-4-ANEPPS (15 μM, Molecular Probes, OR, USA) and then administered cytochalasin D (6 μM) to ensure that motion artefact was prevented. Optical APs were recorded with high spatial (0.9 mm), temporal (1.0 ms), and voltage (0.5 mV) resolutions from cells spanning the entire LV wall. AP alternans was induced by decreasing pacing cycle lengths until 1-to-1 capture was lost.

2.3 Ca^{2+} imaging in myocytes

Myocytes were isolated from LV mid-myocardial wall by using standard techniques as described previously.[20] In the VF group, cells were isolated from region located at least 6–8 cm from the centre of the infarct to exclude necrotic and border zone area. Whole-cell patch-clamp recordings of AP and Ca^{2+} currents (I_{Ca}) were performed with an Axopatch 200B amplifier (Axon Instruments, CA, USA). Intracellular Ca^{2+} imaging was performed using an Olympus Fluoview 1000 confocal microscope in line-scan or XY mode. Intra-SR Ca^{2+} levels were studied by loading myocytes with 10 μM Fluo-5N AM (Molecular Probes) for 3–4 h at 37°C. Rhod-2 or Fluo-3 Ca^{2+} indicators were used to monitor cytosolic Ca^{2+}. To facilitate $[Ca^{2+}]_{SR}$ measurements, voltage-clamp experiments involving $[Ca^{2+}]_{SR}$ recordings were performed in the presence of 100 nM isoproterenol (Iso, Calbiochem, CA, USA), a β-adrenergic agonist, which enhances SR Ca^{2+} release by increasing I_{Ca} and stimulating SERCA activity in both control and VF myocytes (see Supplementary material online, *Figure S1*).

2.4 Measurements of ROS production and RyR free thiol content

Changes in ROS production were measured with the fluorescent indicator 5-(and-6) chloromethyl-2′,7′-dichlorodihydrofluoroscein diacetate (DCFDA, 10 μM, Molecular Probes).[21] After subtraction of background fluorescence, the signal (ΔF) was normalized to maximum fluorescence attained by application of 10 mM H_2O_2 (F_{MAX}).

The content of free thiols in RyRs was determined with monobromobimane (mBB, Calbiochem) fluorescence method.[22] Heavy SR vesicles were prepared from fresh tissue samples from control and VF hearts under non-reducing conditions.[23] Samples were incubated with 400 μM mBB for 1 h in the dark at room temperature; subsequently, proteins were acetone precipitated and subjected to SDS–PAGE (4–20% gradient gel, Bio-Rad, CA, USA). mBB fluorescence was normalized to RyR amount determined using Coomassie Blue staining of the gels run in parallel.

2.5 Data analysis

Results are presented as mean ± SE. Statistical significance was evaluated either by the appropriate Student's *t*-test or by one-way ANOVA where appropriate. A *P*-value of <0.05 was considered significant.

3. Results

3.1 AP alternans in wedge preparations

In order to examine potential arrhythmogenic mechanisms in the post-infarction hearts of dogs susceptible to VF, optical APs were recorded from the transmural wall of LV wedge preparations while alternans was induced. The rate-dependence of APD alternans was significantly shifted towards slower heart rates, and the alternans magnitude was increased in wedges from VF animals compared with controls, indicating greater susceptibility to APD alternans in these preparations (*Figure 1A–C*). Furthermore, spatially discordant alternans occurred in all VF wedge preparations but in only 50% of the control. The presence of spatially discordant alternans significantly increased maximum repolarization gradients in VF wedge preparations from 4.3 ± 2.0 to 13.5 ± 3.3 mm/ms ($P < 0.03$). In addition, rapid

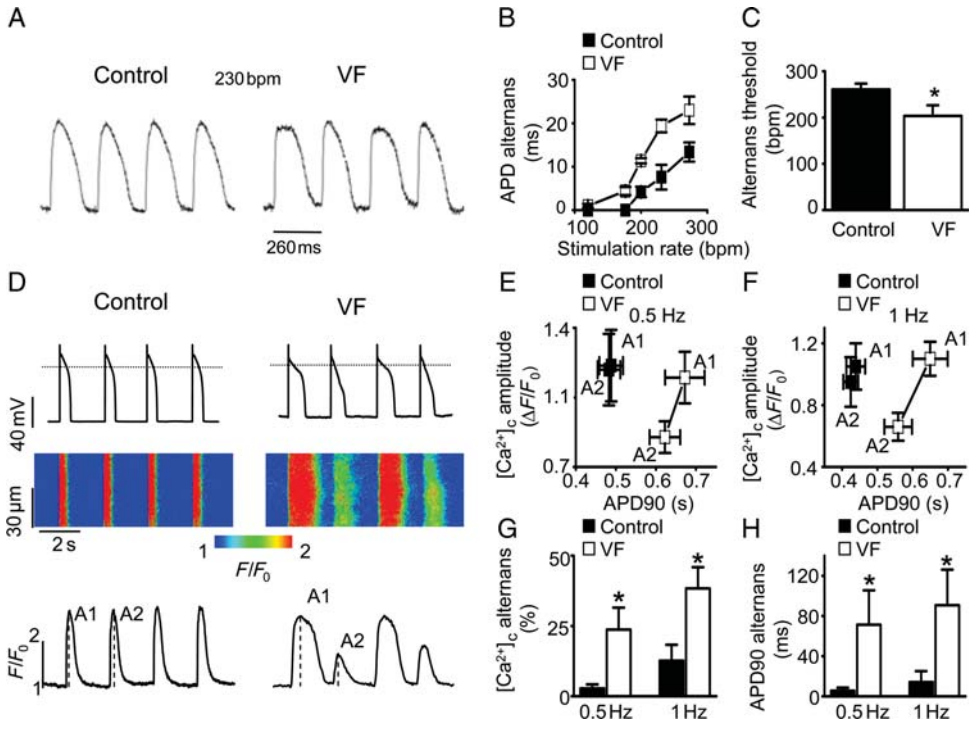

Figure 1 Increased susceptibility to AP and Ca^{2+} alternans in VF hearts. (*A*) Representative mid-myocardial APs recorded at a stimulation rate of 230 bpm from a control and VF heart. (*B*) Dependence of the amplitude of APD alternans on stimulation rate recorded in VF and control wedge preparations. (*C*) APD alternans threshold in VF hearts (203 $\pm$ 23 bpm) is significantly lower than the threshold recorded in control (261 $\pm$ 12 bpm; $^*P < 0.05$ vs. control). (*D*) Representative recordings of membrane potential with corresponding line-scan images and temporal profiles of Fluo-3 fluorescence in control and VF myocytes. (*E* and *F*) Average amplitudes of $[Ca^{2+}]_c$ and duration of corresponding APs were measured with consecutive stimuli in control and VF cells paced with 0.5 and 1 Hz, respectively. A1 and A2 are $[Ca^{2+}]_c$ amplitudes of two consecutive stimuli, as shown in (*D*). Average amplitudes of $[Ca^{2+}]_c$ (*G*) and APD90 (*H*) alternans in control and VF myocytes were measured at indicated stimulation frequencies. $^*P < 0.05$, vs. control.

pacing-induced VF was only observed in the VF preparations, never in control (see Supplementary material online, *Figure S2*). Baseline APD was similar in wedges from hearts of both control (254 $\pm$ 15 ms) and VF (262 $\pm$ 14 ms, P = NS) animals. Conduction velocity in control wedges (0.43 $\pm$ 0.06 m/s) was also similar to that in VF wedges (0.41 $\pm$ 0.06 m/s, P = NS). These results suggest that cardiac alternans is a potential mechanism for arrhythmogenesis in the myocardium of VF animals.

3.2 AP and Ca^{2+} alternans in isolated cardiomyocytes myocytes

Experiments performed on isolated myocytes demonstrated that APD alternans was paralleled by, and occurred in phase with, alternations in the amplitude of Ca^{2+} transients, i.e. Ca^{2+} alternans (*Figure 1D–H*). Consistent with the results in wedge preparations, myocytes from VF hearts showed AP alternans at slower stimulation frequencies than controls.

To explore the mechanisms of Ca^{2+} alternans, the next series of experiments were performed under voltage-clamp conditions (*Figure 2*). Additionally, in these experiments, the role of changes in intra-SR $[Ca^{2+}]$ in the generation of alternans was examined by measuring $[Ca^{2+}]_{SR}$ simultaneously with cytosolic $[Ca^{2+}]$ using SR-entrapped Fluo-5N and cytosolic Rhod-2. Representative cytosolic Ca^{2+} and $[Ca^{2+}]_{SR}$ measurements in a control and VF myocyte paced at 1 Hz are shown in *Figure 2A*. Cytosolic Ca^{2+} alternans in both control and VF cells occurred in phase with changes in diastolic $[Ca^{2+}]_{SR}$. Alternans was more pronounced and occurred at substantially lower $[Ca^{2+}]_{SR}$ in VF cells than in controls. These results obtained at a fixed membrane potential showed that changes in Ca^{2+} handling alone could produce Ca^{2+} and, therefore, APD alternans. These data also point to a role for $[Ca^{2+}]_{SR}$ fluctuations in the genesis of Ca^{2+} alternans.

Increased steepness of the Ca^{2+} release–load relationship is thought to be a key factor contributing to the development of Ca^{2+} alternans,[11,14] although the contribution of this mechanism has been recently challenged.[12] We measured directly the steepness of release–load relationships in control vs. VF myocytes exhibiting Ca^{2+} alternans. EC coupling gain, defined as the Ca^{2+} transient amplitude normalized to the peak of corresponding I_{Ca} density, was plotted as a function of the end-diastolic $[Ca^{2+}]_{SR}$ of the preceding Ca^{2+} release cycle for the large and small releases in control and VF myocytes (*Figure 2*). As shown in *Figure 2B* and *C*, the steepness of Ca^{2+} release–load relationship was markedly increased in VF cells compared with control cells.

3.3 Ca^{2+} release during EC coupling

To better understand the mechanism(s) responsible for altered cellular Ca^{2+} dynamics in myocytes from the hearts of animals susceptible to VF, SR Ca^{2+} release in control vs. VF myocytes was characterized in more detail. *Figure 3A* shows representative recordings of changes in cytosolic and SR Ca^{2+} concentrations along with I_{Ca} during steps to varying membrane potentials in a control and a VF myocyte. The results are summarized in *Figure 3B* and *C* that plot the voltage dependencies of the peak amplitude of cytosolic Ca^{2+} transients, the nadir of the luminal Ca^{2+}

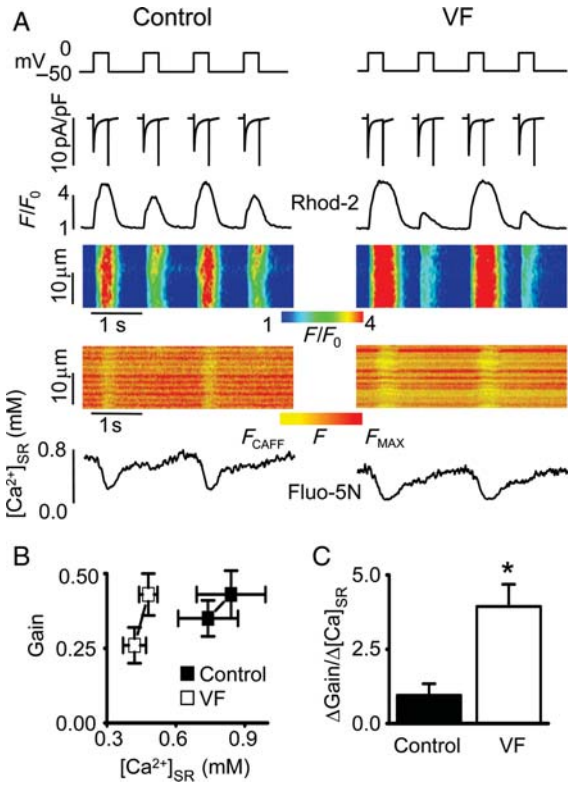

Figure 2 Properties of SR Ca^{2+} release in control and VF myocytes displaying Ca^{2+} alternans during 1 Hz stimulation. (*A*) Representative I_{Ca} traces and corresponding line-scan images and temporal profiles of Rhod-2 and Fluo-5N fluorescence recorded in voltage-clamped control and VF cells. Upper traces show voltage protocol used. (*B*) Dependence of the SR Ca^{2+} release gain function ($[Ca^{2+}]_c$ amplitude/density of peak I_{Ca}) on $[Ca^{2+}]_{SR}$ measured with consecutive stimuli in control and VF cells paced at 1 Hz. (*C*) The slope of gain–$[Ca^{2+}]_{SR}$ function, calculated from the data presented in (*B*), was 1.0 ± 0.4 ($n = 9$) in control and 3.9 ± 0.8 ($n = 10$) in VF myocytes, respectively. $^*P < 0.05$ vs. control.

depletion signals, and I_{Ca} amplitude for the control and VF groups. Peak and decay of I_{Ca} measured at 0 mV were similar between the two groups (see Supplementary material online, *Table S1*). The amplitude of maximum cytosolic Ca^{2+} transients (at 0 mV) was also preserved in VF myocytes, although diastolic $[Ca^{2+}]_{SR}$ was markedly reduced from 1.1 ± 0.3 ($n = 7$) observed in control to 0.4 ± 0.1 mM ($n = 8$, $P < 0.05$). Notably, the magnitudes of both the cytosolic and luminal Ca^{2+} signals increased with small depolarizations, resulting in flattened and broadened voltage-dependence curves. *Figure 3D* shows that the ratio of gain of Ca^{2+}-induced Ca^{2+} release to $[Ca^{2+}]_{SR}$ is significantly increased in VF myocytes, suggesting that RyR functional activity was increased in VF myocytes during EC coupling.

3.4 Ca^{2+} sparks and SR Ca^{2+} leak

In order to examine further the relationship between susceptibility to VF and SR Ca^{2+} release, Ca^{2+} sparks were measured in permeabilized myocytes at a constant baseline cytosolic $[Ca^{2+}]$ (see Supplementary material online, *Figure S3*). Ca^{2+} spark frequency was significantly increased, whereas the amplitude of the Ca^{2+} sparks was significantly decreased in VF myocytes compared with controls. These effects were associated with decreased SR Ca^{2+} content, as determined by applications of caffeine (see Supplementary material online, *Figure S3D* and *E*). Increased Ca^{2+} spark frequency observed at reduced SR Ca^{2+} content suggested that RyR functional activity was enhanced, resulting in leaky SR Ca^{2+} stores in VF myocytes.

3.5 SERCA-mediated SR Ca^{2+} uptake and Na^+/Ca^{2+} exchanger activity

In addition to elevated SR Ca^{2+} leak, the reduced SR Ca^{2+} content in VF myocytes could result from the inhibition of SR Ca^{2+} uptake. SERCA-mediated SR Ca^{2+} uptake was measured in permeabilized control and VF myocytes using SR-entrapped Fluo-5N in the presence of the RyR-antagonist ruthenium red (RR). In these experiments, the SR was first depleted in a Ca^{2+}-free solution using caffeine (10 mM) and then SR Ca^{2+} uptake was initiated by addition of 500 nM Ca^{2+} to the bath solution. As shown in Supplementary material online, *Figure S3F* and *G*, the rate of SR Ca^{2+} uptake measured as an increase in Fluo-5N fluorescence did not significantly differ between control and VF myocytes. Thus, the intrinsic Ca^{2+} transport activity of SERCA was not altered in VF myocytes.

In large animals, Na^+/Ca^{2+} exchanger (NCX) contributes significantly to intracellular Ca^{2+} dynamic and hence it could contribute to the generation of Ca^{2+} alternans. NCX activity was assessed by analysing decay kinetics of caffeine-induced Ca^{2+} transients in control and VF myocytes. As shown in Supplementary material online, *Figure S4*, the rate of decay of caffeine-induced Ca^{2+} transients was not different between control and VF myocytes.

3.6 Role of redox modification of RyR

Redox modification of Ca^{2+} regulatory proteins, including RyRs, is increasingly recognized as a potential factor in the pathophysiology of cardiac diseases, including arrhythmias.[16,24] The levels of ROS in VF and control myocytes were assessed using the ROS-sensitive indicator DCFDA. As shown in *Figure 4A* and *B*, ROS production was increased approximately two-fold in VF myocytes compared with controls. Furthermore, measurements with mBB revealed decreased levels of free thiols in RyRs isolated from VF hearts, providing direct evidence of enhanced oxidation of RyRs in VF hearts. RyRs from each group were treated with a specific oxidizer of sulfhydryl groups, 2,2′-dithiodipyridine (DTDP, 200 μM), to assess susceptibility to oxidation or the reducing agent dithiothreitol (DTT, 5 mM) to assess reversibility of oxidation (*Figure 4C* and *D*).

To determine the functional impact of redox modifications on altered SR Ca^{2+} regulation in VF myocytes, the effects of the reducing agent DTT on SR Ca^{2+} leak were examined in permeabilized VF vs. control myocytes (*Figure 5*). In these experiments, SR Ca^{2+} leak was estimated as the difference in intra-SR $[Ca^{2+}]$ measured with SR-entrapped Fluo-5N in the presence and absence of RR. Since at steady state, $[Ca^{2+}]_{SR}$ is determined by the balance between SR Ca^{2+} leak via RyRs and Ca^{2+} uptake by SERCA, inhibition of RyRs by RR must raise $[Ca^{2+}]_{SR}$ to a degree proportional to the level of Ca^{2+} leak via these channels.[25] Consistent with the results of the Ca^{2+} spark measurements, SR Ca^{2+} leak was significantly higher in VF myocytes than in control (*Figure 5C*). However, treatment of VF cells with the reducing agents DTT or mercaptopropionylglycine (MPG) produced a substantial decrease in leak towards normal levels (*Figure 5A–C*). These results

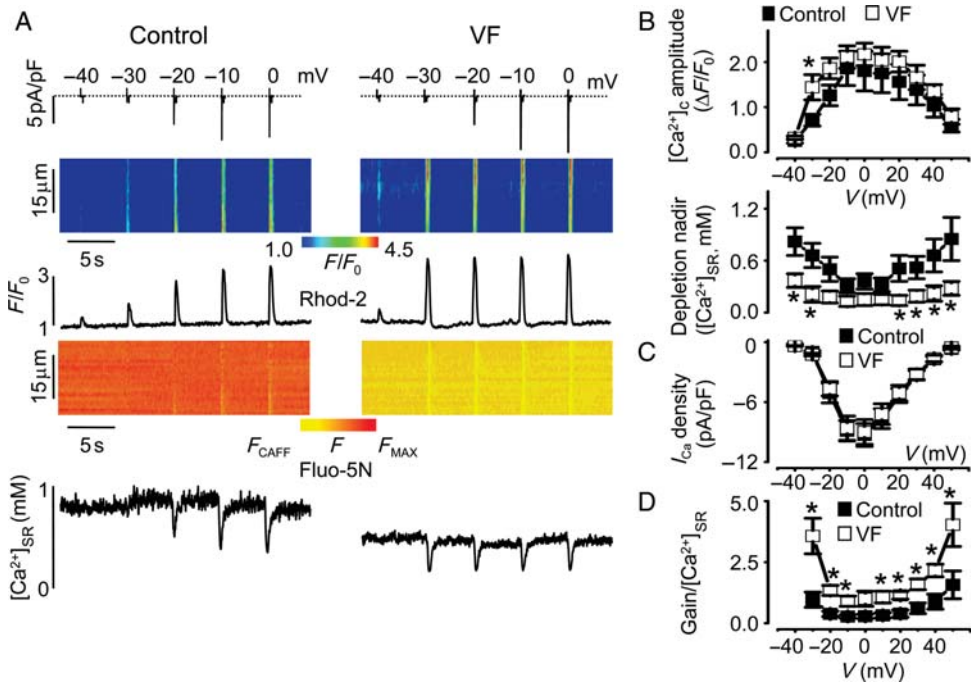

Figure 3 Voltage-dependent characteristics of Ca^{2+}-induced Ca^{2+} release in control and VF myocytes. (*A*) Representative traces of I_{Ca}, line-scan images and temporal profiles of Rhod-2 and Fluo-5N fluorescence recorded in control and VF cells. I_{Ca} and corresponding $[Ca^{2+}]_c$ were evoked by depolarizing steps from a holding potential of −50 mV to the indicated potentials. (*B*) Voltage-dependence of the amplitude of $[Ca^{2+}]_c$ and nadir of SR Ca^{2+} depletion in control and VF cells.*$P < 0.05$ vs. control. Voltage-dependence of the peak I_{Ca} (*C*) and of the gain/diastolic $[Ca^{2+}]_{SR}$ ratio (*D*). *$P < 0.05$ vs. control.

suggest that RyR-mediated SR Ca^{2+} leak was in part attributable to oxidation of RyRs. Moreover, incubation of intact VF myocytes with the antioxidant MPG led to a marked reduction in the amplitude of Ca^{2+} alternans, restoration of diastolic $[Ca^{2+}]_{SR}$ (*Figure 6A–C*), and normalization of the steepness of Ca^{2+} release–$[Ca^{2+}]_{SR}$ relationship (*Figure 6D* and *E*).

4. Discussion

In the present study, the role of, and mechanisms responsible for, abnormal intracellular Ca^{2+} handling in arrhythmogenesis was investigated using a canine model of post-MI SCD with a combination of methodological approaches, including AP mapping in cardiac tissue and monitoring Ca^{2+} levels in the cytosolic and SR compartments of isolated patch-clamped myocytes. The major findings of the present study are as follows: (i) myocytes and tissue obtained from the hearts of animals susceptible to VF exhibited an increased predisposition to arrhythmogenic AP and Ca^{2+} alternans; (ii) these alternans were associated with increased steepness of the Ca^{2+} release–$[Ca^{2+}]_{SR}$ load relationship and hyperactive RyRs; and (iii) the pathological changes in RyRs and in alternans were at least partly due to redox modification(s) of the RyR channel.

4.1 The model

A well-characterized canine model of SCD was used in the present study.[17] This model confers significant advantages over other models, in that it is a large animal model of chronic duration. The model mimics many of the pathological conditions that have been associated with a high risk of SCD including pre-existing ischaemic myocardial injury (i.e. anterior wall MI), acute MI at a site distant from previous ischaemic injury, and altered cardiac autonomic balance (decreased parasympathetic regulation coupled with enhanced sympathetic activation).[17] In addition, it is essential that the lethal arrhythmias must be reliably and reproducibly induced before an accurate assessment of the mechanism responsible for these malignant rhythm disorders can be determined. In this model, VF is reproducibly induced in 95% of animals.[17] Thus, the model used in this study provides the opportunity to investigate the relationship between pathological alterations in Ca^{2+} regulation and the propensity for lethal ventricular arrhythmias following MI in the absence of heart failure.

4.2 Role and mechanisms of Ca^{2+} alternans

Ca^{2+} alternans is increasingly recognized as an important factor in the development of cardiac arrhythmias by generating a substrate for re-entrant excitation.[6,26,27] In the present study, myocytes and tissue obtained from the hearts of animals susceptible to VF exhibited an increased propensity for APD and Ca^{2+} alternans. The underlying factors responsible for Ca^{2+} alternans have not been fully determined, especially in the setting of cardiac disease. Several mechanisms have been suggested, including slowed SERCA-mediated SR Ca^{2+} uptake,[10,11] incomplete recovery of RyR from inactivation,[12,13] and increased steepness of the Ca^{2+} release–SR Ca^{2+} load relationship.[11,14] The relative importance of these mechanisms is currently subject to debate. The effect of slowed Ca^{2+} uptake and prolonged refractoriness would be to decrease Ca^{2+} cycling such that normal Ca^{2+} release from the SR could be obtained only on alternating beats. With a steep Ca^{2+} release–load relationship, which, in general, reflects the stimulatory effects of luminal Ca^{2+} on RyR open probability,[28] small differences in $[Ca^{2+}]_{SR}$ would be expected to lead to

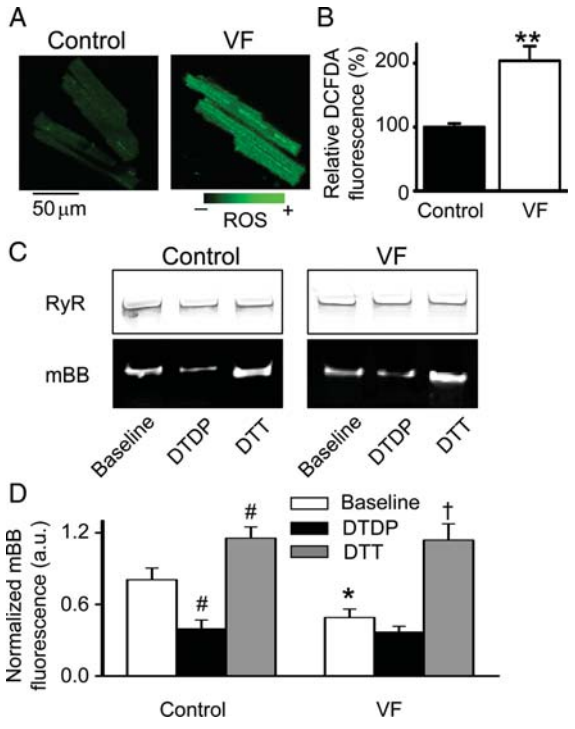

Figure 4 Increased production of ROS and RyR oxidation in VF hearts. (*A*) Representative images of ROS-sensitive indicator DCFDA loaded into myocytes from normal and VF hearts. (*B*) Relative normalized DCFDA fluorescence in myocytes from control ($n = 25$) and VF hearts ($n = 31$). $^{**}P < 0.01$ vs. control. Fluorescence values were normalized to the signal measured in the presence of 10 mM of H_2O_2 and presented relative to control (100%). (*C*) Representative Coomassie Blue-stained gels (upper panels) and corresponding mBB fluorescence intensity (lower panels) of RyR from normal and VF hearts measured under baseline conditions and after 30 min incubation with of 0.2 mM DTDP or 5 mM DTT. (*D*) Relative free thiol content of RyRs from control vs. VF samples obtained by normalizing mBB fluorescence to RyR amount determined using Coomassie Blue staining of the gels run in parallel. $^{*}P < 0.05$ baseline VF ($n = 7$) vs. baseline control ($n = 9$); $^{\#}P < 0.05$ vs. baseline control; $^{\dagger}P < 0.05$ vs. baseline VF.

substantial differences in the amplitude of Ca^{2+} transients, i.e. alternans. In our study, VF-related Ca^{2+} alternans was not attributable to slowed SR Ca^{2+} uptake. SR Ca^{2+} uptake rates were similar in control and VF myocytes (see Supplementary material online, *Figure S3F* and *G*). Moreover, Ca^{2+} alternans persisted in VF cells even after exposure to isoproterenol, which induced a significant acceleration of Ca^{2+} transient decay indicative of accelerated SR Ca^{2+} uptake (*Figures 2* and *6*). Similarly, a slowed recovery of RyR from inactivation did not contribute to alternans. Indeed, the present study demonstrated that both diastolic SR Ca^{2+} release and RyR functional activity were enhanced rather than decreased, consistent with reduced rather than increased inactivation of RyRs. At the same time, supporting a central role for $[Ca^{2+}]_{SR}$-dependent mechanisms in the genesis of alternans, cytosolic Ca^{2+} transients always alternated in phase with changes in end-diastolic $[Ca^{2+}]_{SR}$. Moreover, during Ca^{2+} alternans at a given pacing rate, smaller alterations in end-diastolic $[Ca^{2+}]_{SR}$ resulted in larger deviations in cytosolic Ca^{2+} transients (i.e. steeper Ca^{2+} release–$[Ca^{2+}]_{SR}$ relationship) in VF myocytes than in control myocytes. Thus, altered $[Ca^{2+}]_{SR}$-dependence of release contributed to the increased predisposition to alternans in VF myocytes. Although these studies demonstrate the role of abnormal Ca^{2+} release in the genesis of alternans in our particular arrhythmia model, they do not rule out the possibility that other mechanisms, including defective SR Ca^{2+}-reuptake, contribute to alternans in other disease settings. It is also important to note that even though we show significant abnormalities of Ca^{2+} regulation that can create a substrate for arrhythmogenesis, this does not exclude the possibility that repolarization abnormalities (independent of Ca^{2+}) also contribute to arrhythmogenic events.[20,29]

4.3 Alterations in Ca^{2+} release properties

The present investigation of EC coupling and SR Ca^{2+} release properties provides further insights as to the abnormalities of SR Ca^{2+} signalling in VF myocytes. Our experiments showed that while maximum Ca^{2+} transient amplitude (at 0 mV) was retained, the amplitude of Ca^{2+} transients at low membrane depolarizations was significantly increased, resulting in distinct broadening and flattening of the voltage-dependence of SR Ca^{2+} release in VF myocytes (*Figure 3A* and *B*). Furthermore, diastolic $[Ca^{2+}]_{SR}$ was significantly reduced in VF cells resulting in a significant increase in EC gain at a given intra-SR $[Ca^{2+}]$ (*Figure 3D*). Additionally, VF myocytes exhibited a significantly higher RyR-mediated diastolic SR Ca^{2+} leak measured both as Ca^{2+} sparks (see Supplementary material online, *Figure S3*) and as the ruthenium red-sensitive component of baseline $[Ca^{2+}]_{SR}$ (*Figure 5*). These results indicate that SR Ca^{2+} release via RyRs was potentiated in VF myocytes during both systole and diastole. RyRs are known to respond positively to elevated luminal Ca^{2+}.[28] Our finding that the increase in RyR functional activity occurred against the backdrop of reduced $[Ca^{2+}]_{SR}$ is consistent with the hypothesis that RyR responsiveness to luminal Ca^{2+} was increased in VF myocytes. These changes in RyRs could account for, or contribute to, the increased steepness of release–$[Ca^{2+}]_{SR}$ relationship in VF myocytes during Ca^{2+} alternans.

In previous studies, severe and/or large infarctions resulted in diminished rather than enhanced SR Ca^{2+} release. For example, myocytes from the border zone of infarcted hearts and myocytes from hearts with ischaemic cardiomyopathy[30–33] have been reported to have reduced and slowed Ca^{2+} transients, lowered EC coupling gain, and decreased contractility at all membrane potentials in stark contrast to our present findings. These different results suggest that responses to infarction are more heterogeneous and diverse than previously thought and may reflect different stages of cardiac remodelling following infarction and/or qualitatively different types of responses to infarctions of different severities. It is also possible that changes in RyR in the previous studies were masked by other changes such as disruption of the membrane system in models with more severe/larger infarction that induced heart failure. Notably, our model does not exhibit impaired LV systolic function and is a model of arrhythmogenesis without concomitant heart failure.[17,20]

4.4 Role of RyR redox modification in altered SR Ca^{2+} release

In the present study, we investigated the hypothesis that abnormal RyR function in VF hearts results from redox modification of the channel protein. This hypothesis was based on the following notions. Sulfhydryl oxidation of reactive cysteine molecules by various oxidizing agents is known to

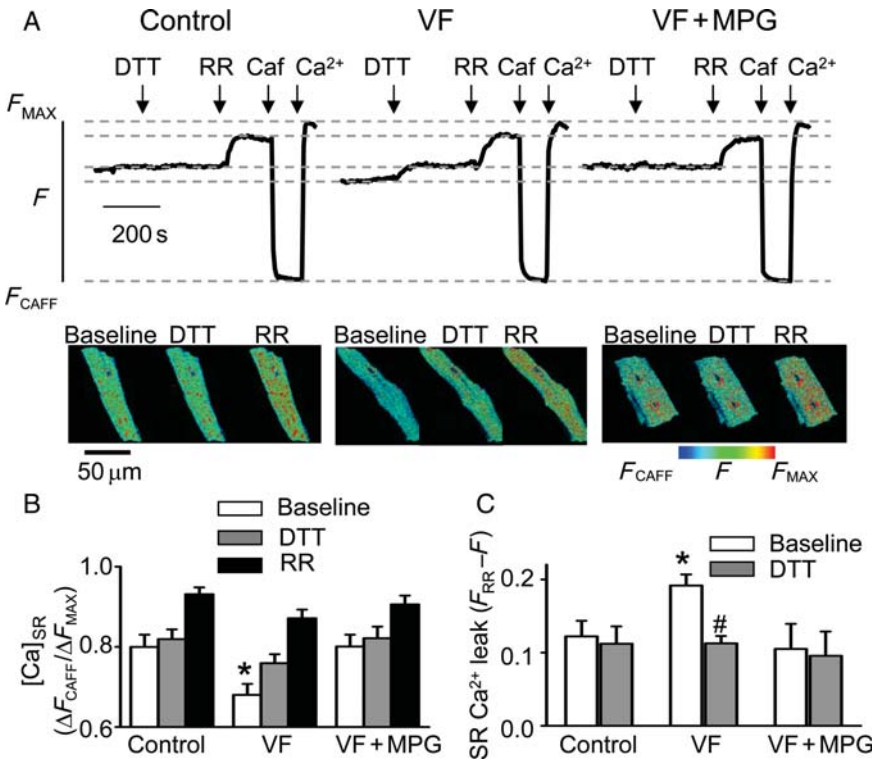

Figure 5 Reducing agents normalize $[Ca^{2+}]_{SR}$ in permeabilized VF myocytes by inhibiting RR-sensitive SR Ca^{2+} leak. (*A*) Time-dependent profiles of intra-SR Fluo-5N signals recorded before and after the application of 1 mM DTT and 30 μmol/L RR in control, VF cells, and in VF cells pre-treated with 1 mM *N*-(2-mercapto-propionyl)glycine (MPG). Representative XY-images of Fluo-5N signal of a control, a VF cell, and a VF cell pre-treated with MPG recorded under specified conditions. (*B*) Average data of normalized Fluo-5N signal in control ($n = 11$), VF cells ($n = 12$), and VF cells pre-treated with MPG ($n = 9$) recorded in the absence and presence of DTT and RR. $^{*}P < 0.05$ baseline VF vs. baseline control and VF with MPG. (*C*) SR Ca^{2+} leak, defined as the difference in Fluo-5N fluorescence recorded with (F_{RR}) and without (F) RR, under baseline conditions and in the presence of DTT in control, VF, and MPG-treated VF myocytes. $^{*}P < 0.05$ vs. baseline control; $^{\#}P < 0.05$ vs. baseline VF.

increase RyR open time probability, thus producing 'leaky' RyR channels.[16] Previous studies demonstrated increased ROS production and oxidative stress in various ischaemic and non-ischemic cardiac diseases states[15] including models of healed infarction (up to 16 weeks post-MI).[34] In the present study, the following findings are consistent with redox-mediated alterations of Ca^{2+} signalling in VF hearts: (i) ROS generation was enhanced in VF myocytes (*Figure 4A* and *B*); (ii) the number of free thiols on RyRs decreased in VF hearts compared with control (*Figure 4C* and *D*); and (iii) reducing agents normalized Ca^{2+} leak and Ca^{2+} cycling in VF myocytes (*Figures 5* and *6*).

Even though treatment with antioxidants resulted in significant improvements in intracellular Ca^{2+} handling, the results of the present study do not exclude the possibility that other types of post-translational modification(s), such as phosphorylation by cAMP-dependent protein kinase[35,36] and/or Ca^{2+}/calmodulin kinase II,[37] also contribute to abnormal Ca^{2+} handling in VF cells. Moreover, these pathways may be linked at the level of CAMKII, which is reportedly activated by increased oxidative stress and contributes to ischaemic myocardial apoptosis[38] and arrhythmogenesis.[39]

4.5 Arrhythmia mechanisms

Previous work illustrated a role for re-entry in the pathogenesis of ventricular tachyarrhythmias in this model.[40] In addition, Ca^{2+} chelators (BAPTA-AM) and modulators of Ca^{2+} entry (e.g. L-type Ca^{2+} channel blockers) have demonstrated *in vivo* efficacy in preventing tachyarrhythmias in this model.[17,40,41] Importantly, both have also been shown to inhibit Ca^{2+} alternans.[5] The results from the present study are consistent with these previous *in vivo* observations and provide further insights into arrhythmogenic mechanisms in the post-MI heart. Our tissue and myocyte studies demonstrated an increased predisposition to APD and Ca^{2+} alternans in arrhythmic hearts following MI. APD alternans is arrhythmogenic because it can amplify spatial heterogeneities of repolarization, creating a substrate for re-entrant excitation.[42] Of note, the VF wedge preparations in our study showed increased predisposition to the development of spatially discordant alternans that significantly increased spatial gradients of repolarization and is a known precursor to VF.[6,9]

4.6 Limitations

Caution should be used when extrapolating our findings to *in vivo* settings. Our experiments on isolated cardiac myocytes were performed at the room temperature and ambient O_2 tension (20%) as opposed to physiological temperature (37°C) and O_2 (5%) levels which are known to effect both myocyte Ca^{2+} handling and redox reactions. Although our data suggest that alternans is a potential mechanism of arrhythmogenesis in these VF hearts, our study does not preclude the possibility that other mechanisms such as ectopic activity or conduction block due to preserved structural damage (scar) contribute to arrhythmogenesis.

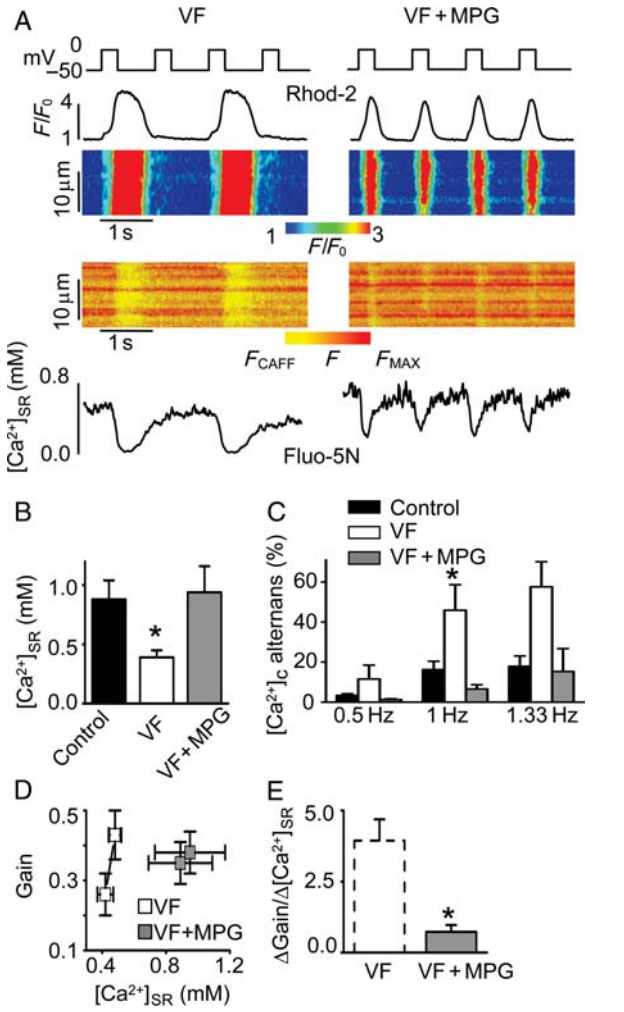

Figure 6 A reducing agent normalizes $[Ca^{2+}]_{SR}$ and lessens the amplitude of Ca^{2+} alternans in patch-clamped VF myocytes. (*A*) Representative line-scan images and temporal profiles of Rhod-2 and Fluo-5N fluorescence recorded in voltage-clamped VF cells recorded in the absence and presence of MPG, a reducing agent. Cells were stimulated at 1 Hz frequency. Upper traces show voltage protocol used. (*B*) Average values of end-diastolic $[Ca^{2+}]_{SR}$ were 0.88 ± 0.16, 0.41 ± 0.06, and 0.94 ± 0.22 mM in control ($n = 8$), in VF myocytes ($n = 10$), and in VF myocytes treated with 750 μM MPG ($n = 9$), respectively. *$P < 0.05$ vs. control. (*C*) Average amplitude of $[Ca^{2+}]_c$ alternans recorded at the indicated frequency of stimulation in voltage-clamped control cells ($n = 4$–13), VF cells ($n = 8$–11), and VF cells treated with MPG ($n = 6$–9). *$P < 0.05$ vs. 1 Hz control and 1 Hz VF cells treated with MPG. (*D*) Dependence of the SR Ca^{2+} release gain function ($[Ca^{2+}]_c$ amplitude/density of peak I_{Ca}) on $[Ca^{2+}]_{SR}$ measured for consecutive stimuli in VF cells in the absence and presence of MPG. Cells were paced at 1 Hz. (*E*) The slope of gain–$[Ca^{2+}]_{SR}$ function, calculated from the data presented (*D*), was 0.7 ± 0.2 ($n = 9$) in VF myocytes treated with MPG. *$P < 0.05$ vs. untreated VF.

4.7 Conclusions

Collectively, our data suggest that redox-dependent changes in RyRs contribute to arrhythmogenesis by promoting Ca^{2+} cycling-induced repolarization alternans. Therefore, in the post-infarction heart, normalizing Ca^{2+} release, potentially via targeted antioxidant therapies, may be beneficial in patients at risk for SCD.

Supplementary material

Supplementary material is available at *Cardiovascular Research* online.

Conflict of interest: none declared.

Funding

This work was supported by the National Institutes of Health Grants [HL074045 and HL063043 to S.G., HL086700 and HL68609 to G.E.B., and HL84142 to K.R.L.].

References

1. Moss AJ, Zareba W, Hall WJ, Klein H, Wilber DJ, Cannom DS *et al*. Prophylactic implantation of a defibrillator in patients with myocardial infarction and reduced ejection fraction. *N Engl J Med* 2002;**346**:877–883.
2. Bunch TJ, Hohnloser SH, Gersh BJ. Mechanisms of sudden cardiac death in myocardial infarction survivors: insights from the randomized trials of implantable cardioverter-defibrillators. *Circulation* 2007;**115**:2451–2457.
3. Clements-Jewery H, Andrag E, Curtis MJ. Druggable targets for sudden cardiac death prevention: lessons from the past and strategies for the future. *Curr Opin Pharmacol* 2009;**9**:146–153.
4. Janse MJ, Wit AL. Electrophysiological mechanisms of ventricular arrhythmias resulting from myocardial ischemia and infarction. *Physiol Rev* 1989;**69**:1049–1169.
5. Walker ML, Rosenbaum DS. Repolarization alternans: implications for the mechanism and prevention of sudden cardiac death. *Cardiovasc Res* 2003;**57**:599–614.
6. Weiss JN, Karma A, Shiferaw Y, Chen PS, Garfinkel A, Qu Z. From pulsus to pulseless: the saga of cardiac alternans. *Circ Res* 2006;**98**:1244–1253.
7. Huser J, Wang YG, Sheehan KA, Cifuentes F, Lipsius SL, Blatter LA. Functional coupling between glycolysis and excitation-contraction coupling underlies alternans in cat heart cells. *J Physiol* 2000;**524**(Pt. 3):795–806.
8. Eisner DA, Li Y, O'Neill SC. Alternans of intracellular calcium: mechanism and significance. *Heart Rhythm* 2006;**3**:743–745.
9. Laurita KR, Rosenbaum DS. Mechanisms and potential therapeutic targets for ventricular arrhythmias associated with impaired cardiac calcium cycling. *J Mol Cell Cardiol* 2008;**44**:31–43.
10. Kameyama M, Hirayama Y, Saitoh H, Maruyama M, Atarashi H, Takano T. Possible contribution of the sarcoplasmic reticulum Ca^{2+} pump function to electrical and mechanical alternans. *J Electrocardiol* 2003;**36**:125–135.
11. Shiferaw Y, Watanabe MA, Garfinkel A, Weiss JN, Karma A. Model of intracellular calcium cycling in ventricular myocytes. *Biophys J* 2003;**85**:3666–3686.
12. Picht E, DeSantiago J, Blatter LA, Bers DM. Cardiac alternans do not rely on diastolic sarcoplasmic reticulum calcium content fluctuations. *Circ Res* 2006;**99**:740–748.
13. Restrepo JG, Weiss JN, Karma A. Calsequestrin-mediated mechanism for cellular calcium transient alternans. *Biophys J* 2008;**95**:3767–3789.
14. Diaz ME, O'Neill SC, Eisner DA. Sarcoplasmic reticulum calcium content fluctuation is the key to cardiac alternans. *Circ Res* 2004;**94**:650–656.
15. Giordano FJ. Oxygen, oxidative stress, hypoxia, and heart failure. *J Clin Invest* 2005;**115**:500–508.
16. Zima AV, Blatter LA. Redox regulation of cardiac calcium channels and transporters. *Cardiovasc Res* 2006;**71**:310–321.
17. Billman GE. A comprehensive review and analysis of 25 years of data from an in vivo canine model of sudden cardiac death: implications for future anti-arrhythmic drug development. *Pharmacol Ther* 2006;**111**:808–835.
18. Billman GE, Schwartz PJ, Stone HL. Baroreceptor reflex control of heart rate: a predictor of sudden cardiac death. *Circulation* 1982;**66**:874–880.
19. Schwartz PJ, Billman GE, Stone HL. Autonomic mechanisms in ventricular fibrillation induced by myocardial ischemia during exercise in dogs with healed myocardial infarction. An experimental preparation for sudden cardiac death. *Circulation* 1984;**69**:790–800.
20. Sridhar A, Nishijima Y, Terentyev D, Terentyeva R, Uelmen R, Kukielka M *et al*. Repolarization abnormalities and afterdepolarizations in a canine model of sudden cardiac death. *Am J Physiol Regul Integr Comp Physiol* 2008;**295**:R1463–R1472.
21. Terentyev D, Gyorke I, Belevych AE, Terentyeva R, Sridhar A, Nishijima Y *et al*. Redox modification of ryanodine receptors contributes to sarcoplasmic reticulum Ca^{2+} leak in chronic heart failure. *Circ Res* 2008;**103**:1466–1472.
22. Xu L, Eu JP, Meissner G, Stamler JS. Activation of the cardiac calcium release channel (ryanodine receptor) by poly-S-nitrosylation. *Science* 1998;**279**:234–237.

23. Hidalgo C, Aracena P, Sanchez G, Donoso P. Redox regulation of calcium release in skeletal and cardiac muscle. *Biol Res* 2002;**35**:183–193.
24. Hidalgo C, Donoso P. Crosstalk between calcium and redox signaling: from molecular mechanisms to health implications. *Antioxid Redox Signal* 2008;**10**:1275–1312.
25. Belevych A, Kubalova Z, Terentyev D, Hamlin RL, Carnes CA, Gyorke S. Enhanced ryanodine receptor-mediated calcium leak determines reduced sarcoplasmic reticulum calcium content in chronic canine heart failure. *Biophys J* 2007;**93**:4083–4092.
26. Weiss JN, Chen PS, Wu TJ, Siegerman C, Garfinkel A. Ventricular fibrillation: new insights into mechanisms. *Ann N Y Acad Sci* 2004;**1015**: 122–132.
27. Laurita KR, Rosenbaum DS. Cellular mechanisms of arrhythmogenic cardiac alternans. *Prog Biophys Mol Biol* 2008;**97**:332–347.
28. Gyorke S, Terentyev D. Modulation of ryanodine receptor by luminal calcium and accessory proteins in health and cardiac disease. *Cardiovasc Res* 2008;**77**:245–255.
29. Biliczki P, Virag L, Iost N, Papp JG, Varro A. Interaction of different potassium channels in cardiac repolarization in dog ventricular preparations: role of repolarization reserve. *Br J Pharmacol* 2002;**137**:361–368.
30. Litwin SE, Bridge JH. Enhanced Na^{+}-Ca^{2+} exchange in the infarcted heart. Implications for excitation-contraction coupling. *Circ Res* 1997; **81**:1083–1093.
31. Kim YK, Kim SJ, Kramer CM, Yatani A, Takagi G, Mankad S *et al*. Altered excitation-contraction coupling in myocytes from remodeled myocardium after chronic myocardial infarction. *J Mol Cell Cardiol* 2002;**34**: 63–73.
32. Gomez AM, Guatimosim S, Dilly KW, Vassort G, Lederer WJ. Heart failure after myocardial infarction: altered excitation-contraction coupling. *Circulation* 2001;**104**:688–693.
33. Heinzel FR, Bito V, Biesmans L, Wu M, Detre E, von Wegner F *et al*. Remodeling of T-tubules and reduced synchrony of Ca^{2+} release in myocytes from chronically ischemic myocardium. *Circ Res* 2008;**102**:338–346.
34. Hill MF, Singal PK. Right and left myocardial antioxidant responses during heart failure subsequent to myocardial infarction. *Circulation* 1997;**96**: 2414–2420.
35. Lindegger N, Niggli E. Paradoxical SR Ca^{2+} release in guinea-pig cardiac myocytes after beta-adrenergic stimulation revealed by two-photon photolysis of caged Ca^{2+}. *J Physiol* 2005;**565**:801–813.
36. Marx SO, Reiken S, Hisamatsu Y, Jayaraman T, Burkhoff D, Rosemblit N *et al*. PKA phosphorylation dissociates FKBP12.6 from the calcium release channel (ryanodine receptor): defective regulation in failing hearts. *Cell* 2000;**101**:365–376.
37. Livshitz LM, Rudy Y. Regulation of Ca^{2+} and electrical alternans in cardiac myocytes: role of CAMKII and repolarizing currents. *Am J Physiol Heart Circ Physiol* 2007;**292**:H2854–H2866.
38. Erickson JR, Joiner ML, Guan X, Kutschke W, Yang J, Oddis CV *et al*. A dynamic pathway for calcium-independent activation of CaMKII by methionine oxidation. *Cell* 2008;**133**:462–474.
39. Xie LH, Chen F, Karagueuzian HS, Weiss JN. Oxidative stress-induced afterdepolarizations and calmodulin kinase II signaling. *Circ Res* 2009; **104**:79–86.
40. Billman GE, Hamlin RL. The effects of mibefradil, a novel calcium channel antagonist on ventricular arrhythmias induced by myocardial ischemia and programmed electrical stimulation. *J Pharmacol Exp Ther* 1996;**277**:1517–1526.
41. Billman GE, McIlroy B, Johnson JD. Elevated myocardial calcium and its role in sudden cardiac death. *FASEB J* 1991;**5**:2586–2592.
42. Pastore JM, Girouard SD, Laurita KR, Akar FG, Rosenbaum DS. Mechanism linking T-wave alternans to the genesis of cardiac fibrillation. *Circulation* 1999;**99**:1385–1394.